ՀԱՅԱՍՏԱՆԻ ԳԻՏՈՒԹՅՈՒՆՆԵՐԻ ԱԶԳԱՅԻՆ ԱԿԱԴԵՄԻԱՅԻ ՏԵՂԵԿԱԳԻՐ
ИЗВЕСТИЯ НАЦИОНАЛЬНОЙ АКАДЕМИИ НАУК АРМЕНИИ

Մեխանիկա 69, №1, 2016 Механика

УДК 593.3

DYNAMIC BIMORPH THERMO-PIEZOELECTRIC BENDERS WITH ARBITRARY SUPPORT LOCATION.

PART I: APPLICATION TO ENERGY HARVESTING-ANALYTICAL DERIVATIONS

Bagdasaryan Gevorg Y. , Hasanyan Armanj D. , Hasanyan Davresh J.

Dedicated to the memory of late Professor Vardges Gnuni

Keywords: Thermo-electro-elastic effects, energy harvesting, resonant frequency, piezoceramic, pyroelectric effect

Ключевые слова: термоэлектроупругий эффект, накопитель энергии, резонансная частота, пьезокерамика, пироэлектрический эффект

Բանալի բառեր. Ջերմաէլեկտրաառաձգականություն, ռեզոնանսային հաճախություն, պիեզոկերամիկա, պիեզոէլեկտրիկ

Багдасарян Г.Е., Асанян А.Д, Асанян Д.Д.

Динамическая двухслойная термоупругая пластина с произвольно расположенными опорами.

Часть I. Применение к накоплению энергии - аналитический вывод.

Приведён подробный теоретический анализ динамического термо-пьезоэлектрического двухслойного накопителя энергии. Учтены пироэлектрические и температурные эффекты расширения. Получено общее аналитическое выражение для коэффициента энергетических преобразований в случае двухслойной пластинки, когда учитываются механические, электрические и температурные поля.

В частном случае получено аналитическое выражение для коэффициента накопителя энергии, обусловленного пироэлектрическим и тепловым расширением.

В качестве частных примеров приводятся результаты для консольной и шарнирно опёртой балок.

Բաղդասարյան Գ.Ե., Հասանյան Ա.Դ., Հասանյան Դ.Ջ

Կամայականորեն տեղակայված հենարաններով երկշերտ ջերմաառաձգական դինամիկական սալ:

Մաս I: Էներգիայի կուտակում – տեսական հետազոտություն

Կատարված է դինամիկ ջերմապիեզոէլեկտրական երկշերտ էներգիայի կուտակիչի մանրակրկիտ տեսական հետազոտություն: Հաշվի են առնված պիրոէլեկտրական և ջերմային էֆեկտները: Ստացված է էներգիայի կուտակիչի գործակցի անալիտիկ արտահայտությունը երկշերտ սալի դեպքում, երբ հաշվի են առնվում մեխանիկական, էլեկտրական և ջերմային դաշտերը: Մասնավոր դեպքում ստացված է էներգիայի կուտակիչի գործակցի անալիտիկ արտահայտությունը՝ պայմանավորված պիրոէլեկտրական և ջերմային ընդարձակմամբ: Որպես մասնավոր օրինակ բերված են արդյունքները կոնսոլային և հոդակապորեն ամրակցված հեծանների համար:

Abstract

A comprehensive theoretical analysis of a dynamic thermo-ferro-electric pre-stressed bimorph energy harvester is performed. The analysis also takes into account pyroelectric and thermal expansion effects. The most general analytical expression for the energy conversation coefficients are presented for bi-layer. These coefficients we derive for more general situation when mechanical, electrical, thermal fields are present. We derive coefficients (transformation coefficients) for sensing, actuating, and energy harvesting. As a particular case, we derive an analytical expression for the energy harvesting coefficient due to pyroelectric and thermal expansion effects in a rater general situation. This is a function of material properties, location of boundary conditions, vibration frequency, and in plane compressive/tensile follower force. Numerical simulations of the analytical results are presented. Effects of volume fraction, material properties, applied mechanical loads, and boundary conditions on the harvesting coefficients are introduced in the figures. The results for a cantilever and a simply-supported plate-layer are obtained as particular cases. The result for a low frequency (static) system is obtained as a particular case by approaching the vibration frequency to zero. It is shown that volume fraction, material properties, plain compressive/tensile follower force, the location of the boundary conditions, and the vibrational frequency of the bimorph strongly influence the

strain distribution, and this in effect influences the charge coefficient and the generation of energy. The proposed model can be extended to thermal energy harvesters of piezoelectric-shape memory alloy (SMA) composites.

1. Introduction

Piezoelectric materials have found widespread applications in the last decade in sensors, actuators, loud speakers, etc. because of their ability to convert electrical energy to mechanical, thermal, and magnetic energy, and vice versa. This has led to an accumulation of research to develop piezoelectric based energy harvesting devices as power generators in a variety of portable and low power consuming devices. The process of extracting energy from the surrounding environment is termed as energy harvesting. Energy harvesting, which originated from the windmill and water wheel, is widely being considered as a low maintenance solution for a wide variety of applications.

Note that energy harvesting techniques are numerous [3, 5-11, 14-16, 18- 20, 22-26]. Photovoltaic-solar energy is directly converted into electrical energy using polarized solar cells (semiconductor devices); mechanical (vibrations), electrostatic method -a relative movement between electrically isolated charged capacitor planes is utilized. The work against the electrostatic force between the plates provides the harvested energy, electromagnetic method – an electromagnetic induction arising from the relative motion (rotation or linear) between a magnetic flux and a conductor is used, piezoelectric method-active materials are employed to generate the energy when mechanically stressed [3, 5-11, 14-16, 18- 20, 22-26].

Other attractive area for harvesting energy is from thermal sources. Thermal energy (temperature gradient) is converted into electrical energy using e.g. Seebeck's effect [10, 24]. Thermal-energy (temperature variation) is converted via the pyroelectric effect [9, 18, 23,26]. Mention that using a thermoelectric module a limited temperature gradient due to the limited heat exchange (Seebeck's effect), a maximum efficiency of ~3-4% can be expected. However, on the contrary, a pyroelectric device may reach efficiency up to 50% of efficiency [3,24].

Vibration energy can be converted into electrical energy through piezoelectric, electromagnetic and capacitive transducers. Among them, piezoelectric vibration-to electricity converters have received much attention, as they have high electromechanical coupling and no external voltage source requirement, and they are particularly attractive for use in MEMS [1, 2, 4, 13,17,21].

Authors in [20] discussed a recent commercial wristwatch that uses thermoelectric modules to generate enough power to run the clock's mechanical components. The thermoelectric modules in the clock work by the thermal gradient produced through body heat. Pyroelectric effect is another possibly for converting heat into electricity. Authors in [9, 16, 23, 26] proposed a pyroelectric energy harvesting using materials such as PZT-5A, PMN-PT, PVDF, and thin-films. It was concluded that with a higher pyroelectric coefficient, more power is generated. Authors [18] proposed a thermal energy harvester with a piezo-shape memory alloy (SMA) composite. The combined electro elastic coupling of the piezoelectric with the thermal response of the SMA was studied.

More details about energy harvesting methods, challenges, and thermal sources, the reader is referred to [3, 10, 18, 22, 26].

A piezoelectric energy harvester in an infinite degree of freedom system is often modeled as a mass+ spring + damper + piezo structure (as a lumped model) together with an energy storage system. This approach is simple but cannot capture all phenomena's specific to distributed system. We model an energy harvester as a distributed system and in particular we show that effect of boundary conditions on energy harvesting coefficient can have a significant influence.

The work presented in the paper deals with the modeling of harvesting from mechanical, electrical (piezoelectric), and thermal (pyroelectric) bi-morph type structures. Also, the influence of boundary condition, in plain conservative follower force, vibration frequency, and material properties on a bimorph energy harvester is analyzed while under a thermal-electrical field. The pyroelectric and thermal expansion coefficients are also considered.
The proposed model for the bimorph can be extended for more general cases, for example: to the composites made of magneto-thermo-electro-elastic shape memory alloy's (SMA).

2. Model and Constitutive Equations

A thermally active thermo-piezoelectric bilayer structure of length 2L and thickness $H = h_p + h_m$, where h_p is the thickness of the piezoelectric layer and h_m is the thickness of the elastic layer is considered. The system of coordinates is chosen in such a way that x_1 axis is directed along the neutral line, the x_2 axis is directed across the width, and the x_3 axis is orthogonal to both of them. For simplicity, the structure is assumed to be a two dimensional x_1 plate-layer, where the field functions depend only on the space coordinates x_1 and x_3. We also consider a piezoelectric layer that is poled in the x_3 direction (Fig. 1a, b).

Furthermore, we assume that

- The material of each layer is linearly elastic,
- The strains and displacements are small,
- The length of the composite is much larger than its total thickness $(L >> H)$,
- The thermal field distribution is constant across each layer,
- Bernoulli's (Kirchhoff's) hypothesis is valid for both layers. The displacement in x_1 and x_3 directions are given as

$$\begin{cases} u_1\left(x_1, x_3\right) = u\left(x_1\right) - x_3 \dfrac{\partial w}{\partial x_1} \\ u_3\left(x_1, x_3\right) = w\left(x_1\right) \end{cases} \tag{1}$$

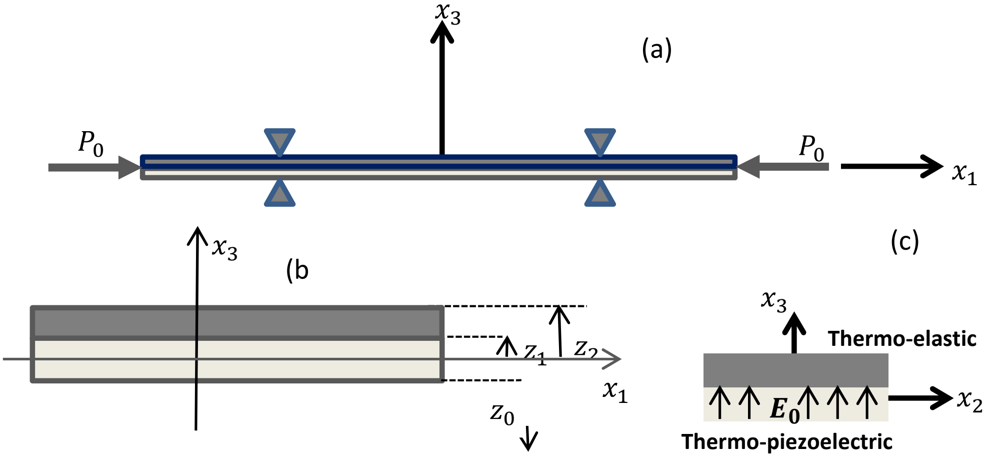

Fig. 1. (a) Thermo-piezoelectric and thermos-elastic bi-layer under thermal field ϑ and a conservative compressive follower force P_0 ; (b) Locations of neutral line from the interfaces; (c) The bi-layer's cross section.

Based on the above assumptions, the equations of motion and Maxwell's electro-magneto static equations for the thermo-elastic and thermo-electro-elastic layers are written as ([1,2,4,13,17,21)

$$T_{ij,i}^{(k)} = \rho^{(k)} \frac{\partial^2 u_j^{(k)}}{\partial t^2} \tag{2}$$

$$D_{i,i}^{(k)} = 0 \quad \text{and} \quad e_{ijm} E_{j,m}^{(k)} = 0, (k = 1, 2), \tag{3a,b}$$

Where $F_{,i} = \frac{\partial F}{\partial x_i}$, T_{ij} is the stress tensor, ρ is the density, D_i is the electric displacement, E_i is the electric field, and e_{ijm} is the permutation index. The superscript "*k*" is used to denote the layer, with *k*=1 indicating the thermo-piezoelectric layer and *k*=2 indicating the thermo-elastic layer.

The constitutive equations are written in a form of

$$\begin{cases} S_i^{(1)} = s_{ij}^{(1)} T_j^{(1)} + d_{ji}^{(1)} E_j^{(1)} + \alpha_i^{(1)} \vartheta \\ D_i^{(1)} = d_{ij}^{(1)} T_j^{(1)} + \varepsilon_{ij}^{(1)} E_j^{(1)} + p_i^{(1)} \vartheta \end{cases} \tag{4}$$

for thermos-pieso-electric layer, where we introduce one index notation for tensors. For example:

two index stress T_{ij} and one index stress T_i related as $T_{11} = T_1,\ T_{22} = T_2, T_{12} = T_6$ and ctr (for details see [9, 12, 13, 17]).

For demonstration purposes only constative equations (4) for $i = 1$ can be written as

$$S_1^{(1)} = s_{11}^{(1)} T_1^{(1)} + s_{12}^{(1)} T_2^{(1)} + s_{13}^{(1)} T_3^{(1)} + d_{31}^{(1)} E_3^{(1)} + \alpha_1^{(1)} \vartheta$$

$$D_1^{(1)} = d_{11}^{(1)} T_1^{(1)} + d_{12}^{(1)} T_2^{(1)} + d_{13}^{(1)} T_3^{(1)} + \varepsilon_{13}^{(1)} E_3^{(1)} + p_1^{(1)} \vartheta$$

For the thermo-elastic layer

$$S_i^{(2)} = s_{ij}^{(2)} T_j^{(2)} + \alpha_i^{(2)} \vartheta \ (i = 1, 6) \tag{5}$$

In these equations, S_i is the strain vector, T_i is the stress vector, ϑ is the thermal field across the two layers, s_{ij} is the compliance matrices of the piezoelectric and pure elastic media, d_{ij} is the piezoelectric coefficient, ε_{ij} is the dielectric permittivity, α_i is the thermal expansion coefficient, and p_i is the pyroelectric coefficient.

Within the scope of Bernoulli's (Kirchhoff's) hypothesis of plate-layer theory, only the strain S_1 is induced in the plate-layer. This strain is given by

$$S_1 = \frac{\partial u_1(x_1, x_3)}{\partial x_1} = \frac{\partial u(x_1)}{\partial x_1} - x_3 \frac{\partial^2 w}{\partial x_1^2} = \varepsilon - x_3 \kappa \tag{6}$$

where $\varepsilon = \frac{\partial u(x_1)}{\partial x_1}$ is a strain along the neutral axis and $\kappa = \frac{\partial^2 W(x_1, t)}{\partial x_1^2}$ is the bending of the neutral axis. Eqn. (6) denotes the linear behavior of the strain S_1 over the entire cross section of the plate-layer and x_3 defines the vertical distance from the neutral axis.

Next, the boundary conditions for the electrical quantities are provided. If there are no electrodes on the surface of the plate-layer and if the layer on these surfaces is in contact with a non-conductive medium (i.e., insulating glue or a vacuum or air), the component of the electric induction vector $D_1^{(1)}$ normal to these surfaces is equal to zero, i.e.

$$D_1^{(1)} = 0 \tag{7}$$

For the electrical field, the following boundary conditions should be satisfie

$$D_3^{(k)}\Big|_{x_3 = z_k} = D_3^{(k+1)}\Big|_{x_3 = z_k}, \quad E_1^{(k)}\Big|_{x_3 = z_k} = E_1^{(k+1)}\Big|_{x_3 = z_k} \tag{8}$$

where $(k = 0, 1, 2)$ and $x_3 = z_k$ is used to denote the location of the interface surfaces as shown in Fig 1. Later, we will assume that the surrounding air is a vacuum. If the electrodes are in a closed circuit condition with a known complex conductivity $Y = Y_0 + iY_1$, then [9, 17]

$$I = \iint \frac{dD_3^{(1)}}{dt} d\Gamma = 2VY \tag{9}$$

Γ is the surface over the electrodes, V is an applied voltage, and I is the magnitude of the current. If the electrodes are in an open circuit condition, then

$$I = \iint \frac{dD_3^{(1)}}{dt} d\Gamma = 0 \tag{10}$$

For the mechanical load on the surface of the plate-layer,

$$\begin{aligned} T_5^{(2)}\Big|_{x_3 = z_2} &= q_1^+, \quad T_5^{(1)}\Big|_{x_3 = z_0} = q_1^-, \\ T_3^{(2)}\Big|_{x_3 = z_2} &= q_3^+, \quad T_3^{(1)}\Big|_{x_3 = z_0} = q_3^- \end{aligned} \tag{11}$$

Where q_i^+ and q_i^- are the forces applied at $x_3 = z_2$ and $x_3 = z_0$. The boundary conditions on the composite edges are provided in the discussion of the vibration of a bilayer composite. In order to construct a theory of plate-layers, some additional assumptions regarding the electrical quantities must be made. As in the theory of piezoelectric shells and plates, the assumed hypotheses depend on the electrical conditions on the surfaces of the composite layers. For the piezoelectric layers, the electric field component $E_3^{(1)}\left(x_1, x_3, t\right)$ will be assumed not to be a function of the coordinates x_1 and x_3, i.e.

$$E_3^{(1)}\left(x_1, x_3, t\right) = E_0(t) \tag{12}$$

Note that more realistic general theory for transversely polarized piezoelectric plates is developed in [2]. Assumption (12) can be interpreted as a particular case from [2].

3. Tangential Force and Bending Moment.

Using the above constitutive relations (4)-(5) and representation (6), we express the induced stresses in the layers of various phases as

$$T_1^{(1)} = \frac{1}{s_{11}^{(1)}}\left(\varepsilon - x_3\kappa - d_{31}^{(1)}E_3^{(1)} - \alpha_1^{(1)}\vartheta\right) \tag{13}$$

for the thermo-piezoelectric layer and

$$T_1^{(2)} = \frac{1}{s_{11}^{(2)}}\left(\varepsilon - x_3\kappa - \alpha_1^{(2)}\vartheta\right) \tag{14}$$

for the thermo-elastic layer. By integrating the stress over the thickness, we obtain the resultant tangential force T_1 as

$$T_1 = \sum_{k=1}^{2}\int_{z_{k-1}}^{z_k} T_1^{(k)}\left(x_1, x_3, t\right)dx_3 = A\varepsilon - B\kappa - A_{01}E_0 - A_\vartheta\,\vartheta \tag{15}$$

where $z_0, z_1 \text{ and } z_2$ are locations of layers surfaces from the mid-plane (in our case it could be neutral plane) with $z_1 - z_0 = h_p$, $z_2 - z_1 = h_m$;

$$B = \frac{z_1^2 - z_0^2}{2s_{11}^{(1)}} + \frac{z_2^2 - z_1^2}{2s_{11}^{(2)}},\ A_{01} = \frac{d_{31}^{(1)}\mathrm{h}_p}{s_{11}^{(1)}},\ A_\vartheta = \frac{\alpha_1^{(1)}\mathrm{h}_P}{s_{11}^{(1)}} + \frac{\alpha_1^{(2)}\mathrm{h}_m}{s_{11}^{(2)}} \tag{16a-c}$$

The bending moment M_1 is calculated according to

$$M_1 = \sum_{k=1}^{2}\int_{z_{k-1}}^{z_k} x_3T_1^{(k)}\left(x_1, x_3, t\right)dx_3 = B\varepsilon - D\kappa - C_1E_0 - C_\vartheta\vartheta \tag{17}$$

where

$$D = \frac{h_p^3}{3s_{11}^{(1)}} + \frac{h_m^3}{3s_{11}^{(2)}},\ C_1 = -\frac{d_{31}^{(1)}h_p^2}{2s_{11}^{(1)}},\ C_\vartheta = \frac{\alpha_1^{(2)}h_m^2}{2s_{11}^{(2)}} - \frac{\alpha_1^{(1)}h_p^2}{2s_{11}^{(1)}} \tag{18a-c}$$

In the context of the above simplification, the second equation in (4) is used to result in

$$D_3 = \int_{-h_p}^{0} D_3^{(1)} dx_3 = C_2 E_0 - C_3 \kappa - P_\vartheta \vartheta \tag{19}$$

Where

$$C_2 = \varepsilon_{33}^{(1)} \left(1 - K_1^2\right) \mathrm{h}_P, \quad C_3 = -\frac{\varepsilon_{33}^{(1)}}{2} h_p^2 \mathrm{r}_1, \quad K_1^2 = \frac{(d_{31}^{(1)})^2}{\varepsilon_{33}^{(1)} s_{11}^{(1)}},$$

$$\mathrm{r}_1 = \frac{d_{31}^{(1)}}{\varepsilon_{33}^{(1)} s_{11}^{(1)}}, \quad P_\vartheta = \left(\frac{\alpha_1^{(1)} d_{31}^{(1)}}{s_{11}^{(1)}} - p_3^{(1)} \right) \mathrm{h}_P. \tag{20a-e}$$

We then combine Eqns (15), (17), (19), and write

$$\begin{cases} A\varepsilon - B\kappa - A_{01} E_0 - A_\vartheta \vartheta = T_1, \\ B\varepsilon - D\kappa - C_1 E_0 - C_\vartheta \vartheta = M_1, \\ \quad C_2 E_0 - C_3 \kappa - P_\vartheta \vartheta = D_3. \end{cases} \tag{21a-c}$$

The unknown function $W(x_1, t)$ should be determined using Eqn. (2), Maxwell's Eqns. (3), and the boundary conditions on the composite edges $x_1 = \pm L.$

Note: From Eq (21) we can see that if the coefficient $B \neq 0,$ then the bending term κ produces a tension T_1 and vise version. These two modes can be decoupled only if $B = 0.$ However, it should be noted that the coefficient B is always zero for symmetric laminated composites. Also, in a general case, this coefficient depends on the choice of the coordinate system, and by choosing the position of the system of coordinates correctly, κ , T_1, ε and M_1 can be decoupled by $B = 0.$ From which we can determine for example z_0 location of system of coordinates from the bottom surface of plate-layer. For pure elastic case such choose give us location of neutral line. In our case (bi layer plate-strip), the z_0 location of the system of coordinates from the bottom surface of bi-layer is

$$z_0 = -\frac{h_p^2 / s_{11}^{(1)} + h_m^2 / s_{11}^{(2)} + 2 h_p h_m / s_{11}^{(2)}}{2\left(h_p / s_{11}^{(1)} + h_m / s_{11}^{(2)}\right)} \quad .$$

In addition to $B = 0$ if we consider also low frequency vibration then longitudinal and transversal motions of plate-layer can be fully decoupled.

4. Equations of Motion of Bilayer Thermo-Electro-Elastic Composite

In plate-layer theory, the equations of motion are obtained by integrating the three-dimensional equations of motion (2)-(3) over the plate-layer thickness. We write the equations of motion in the following form;

$$\begin{cases} \dfrac{\partial T_1}{\partial x_1} + X_1 = \rho \dfrac{\partial^2 u}{\partial t^2} - \tilde{\rho} \dfrac{\partial^3 w}{\partial x_1 \partial t^2} \\ \quad \dfrac{\partial Q}{\partial x_1} + X_3 = \rho \dfrac{\partial^2 w}{\partial t^2} \\ Q = \dfrac{\partial M_1}{\partial x_1} - \tilde{\rho} \dfrac{\partial^2 u}{\partial t^2} - \tilde{\tilde{\rho}} \dfrac{\partial^3 w}{\partial x_1 \partial t^2} \end{cases} \tag{22a-c}$$

Where $\rho = h_P \rho_P + h_m \rho_m$, $\tilde{\rho} = \frac{\rho_1}{2}(z_1^2 - z_0^2) + \frac{\rho_2}{2}(z_2^2 - z_1^2)$,

$\tilde{\tilde{\rho}} = \frac{\rho_1}{3}(z_1^3 - z_0^3) + \frac{\rho_2}{3}(z_2^3 - z_1^3)$, $X_1 = q_1^+ - q_1^-$; q_1^+ and q_1^- are applied shear stresses to the top and bottom of the composite, respectively, $X_3 = q_3^+ - q_3^-$; q_3^+ and q_3^- are the applied normal stresses to the top and the bottom of the composite, respectively.

The total charge Q on each electrode connected to the generator circuit is obtained by integrating the induction D_3 from (9) and (19) over the entire surface of the electrodes Γ. Then, the conduction current is calculated as

$$I = \iint \frac{dD_3^{(1)}}{dt} d\Gamma = 2VY = -\frac{\partial Q}{\partial t} = \frac{\partial}{\partial t}\left(\Gamma C_2 E_0 - \Gamma P_9 \vartheta - C_3 \iint \frac{\partial^2 w}{\partial x_1^2} d\Gamma \right). \tag{23}$$

5. Problem Formulation for a Plate-layer with Arbitrary Support Locations

We assume that the plate-layer occupies the interval $-L \le x_1 \le L$ and is fixed at arbitrary points $x_1 = \pm c$. This plate-layer is subjected to a tangential follower force P_0 at the free ends $x_1 = \pm L$ (see Fig 1). It should be noted that a cantilever plate-layer is obtained for $c = 0$ and a simply-supported plate-layer is obtained for $c = L$.

As we mention above (see paragraph 4, **Note**) by choosing a position of a system of coordinates so that the coefficient $B = 0$ and considering low frequency type of motions, then the bending equation can be decoupled from longitudinal motion and from (22) we can get ([1,2,4,13,17,21])

$$-D \frac{\partial^4 W}{\partial x_1^4} - P_0 \frac{\partial^2 W}{\partial x_1^2} = \rho \frac{\partial^2 W}{\partial t^2} \tag{24}$$

where P_0 is a follower tangential force. Next we are interested in a bilayer's pure bending harmonic motion i.e. $(W(x_1,t), E_0(t), \vartheta(t)) = (w(x_1), E, \theta) e^{i\omega t}$, where ω is the circular frequency of motion. The displacements are denoted as

$$\begin{aligned} w_1(x_1) &= w(x_1) \text{ if } c \le x_1 \le L \\ w_3(x_1) &= w(x_1) \text{ if } -L \le x_1 \le -c \\ w_2(x_1) &= w(x_1) \text{ if } -c \le x_1 \le c \end{aligned} \tag{25a-c}$$

We solve Eqn. (24) with the boundary conditions at $x_1 = \pm L$ and continuity conditions at $x_1 = \pm c$. The boundary conditions at $x_1 = \pm L$ are written as

$$M_1 = -D\frac{d^2 w}{dx_1^2} - C_1 E - C_9 \theta = 0 \text{ and } N = \frac{dM_1}{dx_1} = 0. \tag{26}$$

The continuity conditions yield

$$w_1(c) = w_2(c) = 0,\ w_3(-c) = w_2(-c) = 0,\ \frac{dw_1(c)}{dx_1} = \frac{dw_2(c)}{dx_1},$$

$$\frac{dw_3(-c)}{dx_1} = \frac{dw_2(-c)}{dx_1},\ \frac{d^2 w_1(c)}{dx_1^2} = \frac{d^2 w_2(c)}{dx_1^2},\ \frac{d^2 w_3(-c)}{dx_1^2} = \frac{d^2 w_2(-c)}{dx_1^2}. \tag{27a-f}$$

For simplicity, we will consider the symmetric problem. In this case, $w_3(x_1) = w_1(-x_1)$, $w_2(x_1) = w_2(-x_1)$, and the conditions at $x_1 = -c$ and $x_1 = -L$ (Eqns 27b, d, and f) are replaced by the symmetry conditions

$$\frac{dw_2(0)}{dx_1} = 0,\ \frac{dw_2(0)}{dx_1} = 0. \tag{28}$$

Note that boundary value problem (24)-(28), without thermos-electric properties was discussed in [12] by prof V.Ts. Gnuni (2006).

Next, the following non-dimensional parameters are introduced; $x = x_1 / L,\ \alpha = c / L$,

$$\lambda = \frac{3P_0 L^2 s_{11}^{(1)}}{2h_p^3},\ \Omega^4 = \frac{3\omega^2 L^4 s_{11}^{(1)} \rho_p}{h_p^2},$$

$$p = \left(\left(\left(\frac{\lambda s}{s+h^3} \right)^2 + \frac{\Omega^4 s(1+h\sigma)}{s+h^3} \right)^{1/2} - \frac{\lambda s}{s+h^3} \right)^{1/2} \text{ and}$$

$$q = \left(\left(\left(\frac{\lambda s}{s+h^3} \right)^2 + \frac{\Omega^4 s(1+h\sigma)}{s+h^3} \right)^{1/2} + \frac{\lambda s}{s+h^3} \right)^{1/2},\ \text{where } s = s_{11}^{(2)} / s_{11}^{(1)},$$

$h = h_m / h_p$, and $\sigma = \rho_m / \rho_p$.

The solution of (24) is given by

$$\begin{aligned} w_k(x) = {} & a_{1+4(k-1)} \cosh(px) + a_{2+4(k-1)} \sinh(px) + \\ & + a_{3+4(k-1)} \cos(qx) + a_{4+4(k-1)} \sin(qx) \end{aligned} \tag{29}$$

Where $a_{1+4(k-1)}$, $a_{2+4(k-1)}$, $a_{3+4(k-1)}$ and $a_{4+4(k-1)}$ $(k = 1, 2)$ are unknown coefficients to be determined from the boundary conditions (25)-(28).

Using the boundary conditions (25)-(28) for unknown coefficients a_{1+4k}, a_{2+4k}, a_{3+4k} and a_{4+4k}, $(k = 0, 1)$ the following system of linear algebraic equations are obtained

$$\hat{A} \cdot \vec{X}^T = \frac{L^2}{D} C_1 E \vec{X}_{01}^T + \frac{L^2}{D} C_9 \theta \vec{X}_{01}^T, \tag{30}$$

Where $\vec{X}^T$ and $\vec{X}_{01}^T$ are transposes of

$$\vec{X} = \left(a_1, a_2, a_3, a_4, a_5, a_6, a_7, a_8\right) \text{ and } \vec{X}_{01} = \left(0,0,0,0,0,0,-1,0\right). \tag{31}$$

We also let $\hat{A} =$

$$\begin{pmatrix} 0 & 0 & 0 & 0 & 0 & p & 0 & q \\ 0 & 0 & 0 & 0 & 0 & p^3 & 0 & -q^3 \\ \cosh p\alpha & \sinh p\alpha & \cos q\alpha & \sin q\alpha & 0 & 0 & 0 & 0 \\ 0 & 0 & 0 & 0 & \cosh p\alpha & \sinh p\alpha & \cos q\alpha & \sin q\alpha \\ p\sinh p\alpha & p\cosh p\alpha & -q\sin q\alpha & q\cos q\alpha & -p\sinh p\alpha & -p\cosh p\alpha & q\sin q\alpha & -q\cos q\alpha \\ p^2\cosh p\alpha & p^2\sinh p\alpha & -q^2\cos q\alpha & -q^2\sin q\alpha & -p^2\cosh p\alpha & -p^2\sinh p\alpha & q^2\cos q\alpha & q^2\sin q\alpha \\ p^2\cosh p & p^2\sinh p & -q^2\cos q & -q^2\sin q & 0 & 0 & 0 & 0 \\ p^3\sinh p & p^3\cosh p & q^3\sin q & -q^3\cos q & 0 & 0 & 0 & 0 \end{pmatrix} \tag{32}$$

Assuming $\Delta = \det(\hat{A}) \neq 0$ from (30), we find all unknown coefficients $\vec{X} = \left(a_1, a_2, a_3, a_4, a_5, a_6, a_7, a_8\right)$, i.e.

$$\vec{X}^T = \hat{C} \cdot \frac{1}{\Delta}[\tilde{E}\vec{X}_{01}^T], \tag{33}$$

where the matrix $\hat{C}$ has elements $\hat{C} = (C_{i,j})$ equal to

$\hat{C} = \left(C_{i,j}\right) = \hat{A}^{-1}\det\left(\hat{A}\right) = \hat{A}^{-1}\Delta$ and $\tilde{E} = \dfrac{L^2}{D}C_1 E + \dfrac{L^2}{D}C_9\theta$. The solution (29) is then re-written in the following form

$$w_1(x) = -\frac{v_1}{\Delta}\tilde{E} \text{ and} \tag{34}$$

$$w_2(x) = -\frac{v_2}{\Delta}\tilde{E} \tag{35}$$

The detailed expressions for the coefficients in (34)-(35) are presented in Appendix A. Having the solution for (29) or (34)-(35), we determine the conversion and energy harvesting coefficients for piezoelectric-thermoelastic bimorphs. Under thermodynamic equilibrium, the internal energy density of an infinitesimally small volume element in the piezoelectric material is given by

$$U^p\left(x_1, x_3, t\right) = \frac{1}{2}S_1^{(1)}T_1^{(1)} + \frac{1}{2}E_3^{(1)}D_3^{(1)} \tag{36}$$

Substitution of (6) into (36), and using (4), we obtain

$$U^p\left(x_1, x_3, t\right) = \frac{1}{2s_{11}^{(1)}}(x_3\kappa)^2 + \frac{\alpha_1^{(1)}}{2s_{11}^{(1)}}x_3\kappa\,\vartheta + \frac{C_2}{2h_p}E_0^2 - \frac{P_9}{2h_p}E_0\vartheta, \tag{37}$$

Where $\kappa = \dfrac{\partial^2 W}{\partial x_1^2}$, and C_2 and P_9 are defined in Eq (20a,e). The energy for the thermo-elastic layer is given by

$$U^m\left(x_1, x_3, t\right) = \frac{1}{2}S_1^{(2)}T_1^{(2)} = \frac{1}{2s_{11}^{(2)}}(x_3\kappa)^2 + \frac{\alpha_1^{(2)}}{2s_{11}^{(2)}}x_3\kappa\,\vartheta \tag{38}$$

Once we determine the internal energy density of each layer, the total energy of the bilayer bender is obtained by volume integration. Assuming that the width of the structure is unity, we write

$$U(t)=\int_{-L}^{L}\int_{0}^{h_p}U^{p}dx_3dx_1+\int_{-L}^{L}\int_{-h_m}^{0}U^{m}dx_3dx_1. \tag{39}$$

Using the symmetry conditions $w_3\left(x_1\right)=w_1\left(-x_1\right)$, $w_2\left(x_1\right)=w_2\left(-x_1\right)$, and non-dimensional parameters $x=x_1/L,\ \alpha=c/L,$ Eqn. (39) results in

$$U(t)=C_2LE_0^2-P_\vartheta LE_0\vartheta+\frac{DL}{2}\int_{-1}^{1}k^2dx-\frac{C_\vartheta\vartheta L}{2}\int_{-1}^{1}kdx \tag{40}$$

or using (34)-(35), we write

$$U(t)=\gamma_1E_0^2+\gamma_2\vartheta^2+\gamma_3E_0\vartheta, \tag{41}$$

where $\gamma_i,(i=1,2,3)$ are presented in Appendix B. By treating the electrical and the coupled terms as $U(t)=QV_0$, where $Q(t)$ is the charge and $V_0(t)$ is the voltage, we derive the generated charge by substitution into Eq (41). An expression for the electrical field in terms of voltage $E_0(t)=V_0(t)/h_p$ is obtained. This is differentiated with respect to V_0, where h_p is the distance between the top and the bottom surfaces of the electrodes in the piezoelectric layer as shown in Fig 1. The result is

$$Q(t)=\frac{\partial U\left(t\right)}{\partial V_0}=\frac{2\gamma_1}{h_p^2}V_0(t)+\frac{\gamma_3}{h_p}\vartheta(t)=C_vV_0(t)+Q_\vartheta\vartheta(t), \tag{42}$$

where

$$C_v=\frac{2\gamma_1}{h_p^2}=\frac{2}{h_p^2}(C_2L+\frac{C_1^2L}{D\widehat{\Delta}^2}R_1),$$

$$Q_\vartheta=\frac{\gamma_3}{h_p}=-\frac{P_\vartheta L}{h_p}+\frac{2C_1C_\vartheta L}{h_pD\widehat{\Delta}^2}R_1+\frac{C_1C_\vartheta L}{h_pD\widehat{\Delta}}R_2. \tag{43a,b}$$

The values of R_1 and R_2 are presented in appendix B. Using Eq (43), we determine the amplitude of the generated charge as:

a) from the applied voltage

$$V_0(t)=Ve^{i\omega t}\ ,\ Q_{gen}^{V}=C_vV=\frac{2}{h_p^2}(C_2L+\frac{C_1^2L}{D\widehat{\Delta}^2}R_1)V,\ \text{and} \tag{44a}$$

b) from the thermal gradient $\vartheta=\theta e^{i\omega t}$

$$Q_{gen}^{\vartheta}=Q_\vartheta\theta=(-\frac{P_\vartheta L}{h_p}+\frac{2C_1C_\vartheta L}{h_pD\widehat{\Delta}^2}R_1+\frac{C_1C_\vartheta L}{h_pD\widehat{\Delta}}R_2)\theta. \tag{44b}$$

Recognizing that $Q_{gen}^{V}=C_vV$, the capacitance is

$$C_v=\frac{2}{h_p^2}(C_2L+\frac{C_1^2L}{D\widehat{\Delta}^2}R_1). \tag{45}$$

The generated voltage amplitude from ϑ is

$$V_{gen}^{\vartheta} = \frac{Q_{gen}^{\vartheta}}{C_v}. \tag{46}$$

The generated electrical energy amplitude from ϑ is

$$U_{gen}^{\vartheta} = \frac{1}{2} Q_{gen}^{\vartheta} V_{gen}^{\vartheta}. \tag{47}$$

6. Discussions and Numerical Results.

The non-dimensional thermal energy harvesting coefficient finally derived in the following form

$$\tilde{Q}_{gen}^{\vartheta} = \frac{-s_{11}^{(1)} Q_{gen}^{\vartheta}}{\alpha_1^{(1)} d_{31}^{(1)} L\theta} = (1-\tilde{p}) + \frac{3}{4}\frac{(\alpha_T h^2 - s)}{(s+h^3)}\left(\frac{2R_1}{\widehat{\Delta}^2} + \frac{2R_4}{\widehat{\Delta}}\right), \tag{48}$$

where $\alpha_T = \alpha_1^{(2)} / \alpha_1^{(1)}$, $\tilde{p} = (p_3^{(1)} s_{11}^{(1)}) / (\alpha_1^{(1)} d_{31}^{(1)})$, $h = h_m / h_p$, and $s = s_{11}^{(2)} / s_{11}^{(1)}$.

We can state that expression (48) is derived for the first time in such a general form. In particular, for a static case, assuming also $\alpha_T = 0$ expression (48) coincide with counterpart derived in [18]. The material properties shown in Table 1 will be considered during the numerical simulation of Eqn. (48). It should be noted that the derivation in this work can be extended to the magneto-thermo-electro-elastic shape memory alloy (SMA) composites. For simplicity, the two materials for shape-memory alloy can be also PZT-5A with an aluminum substrate (this case is discussed in [18]).

Using the following properties, the critical bucking load is $\lambda_{\mathrm{cr}} \geq 1.65$. This is determined using the formula for a static Euler's column

$$P_{\mathrm{cr}} = \frac{\pi^2 D}{4L^2}. \tag{49}$$

The value of the follower force will be taken below the critical value.

Numerical results and discussions presented in Part II of this paper.

APPENDIX A

$$v_1 = \omega_1 p^3 \cosh px + \omega_2 q^3 \frac{\cosh px}{\cosh p(1-\alpha)} + \omega_3 p^3 + \omega_4 \frac{q^3}{\cosh p(1-\alpha)},$$

$$v_2 = \omega_5 p^3 \cosh px + \omega_6 pq^2 \frac{\cosh px}{\cosh p(1-\alpha)} + \omega_7 p^3 + \omega_8 \frac{pq^2}{\cosh p(1-\alpha)},$$

$$\widehat{\Delta} = p^3 q^2 \left(\frac{p^2}{q^2 \cosh p(1-\alpha)} + \frac{q^2}{p^2 \cosh p(1-\alpha)} + T\right),$$

$$T = 2\cos q(1-\alpha) - \frac{p\tanh p\alpha + q\tan q\alpha}{q}\sin q(1-\alpha) + \frac{q}{p}\tanh p(1-\alpha)(\sin q(1-\alpha) +$$

$$+ \frac{p\tanh p\alpha + q\tan q\alpha}{q}\cos q(1-\alpha) - \frac{p^2}{q^2}\sin q(1-\alpha)),$$

$$\omega_1 = 1 - \tanh p(1-\alpha)\tanh px,$$

$$\omega_2 = \frac{p}{q}\cos q\left(1-\alpha\right) + (\sin q\left(1-\alpha\right) + \frac{p\tanh p\alpha + q\tan q\alpha}{q}\cos q\left(1-\alpha\right))\tanh px,$$

$$\omega_3 = -\cos qx + \frac{p\tanh p\alpha + q\tan q\alpha}{q}\sin qx + \frac{p}{q}\sin qx\tanh p(1-\alpha),$$

$$\omega_4 = \frac{p}{q}\cos q\left(1-\alpha\right)\left(-\cos qx + \frac{p\tanh p\alpha + q\tan q\alpha}{q}\sin qx\right) -$$

$$\frac{p}{q}\sin qx\left(\sin q\left(1-\alpha\right) + \frac{p\tanh p\alpha + q\tan q\alpha}{q}\cos q\left(1-\alpha\right)\right),$$

$$\omega_5 = 1 + \tanh p\alpha\tanh px,\ \ \omega_6 = \cos q\left(1-\alpha\right)(1 + \tanh p\alpha\tanh px),$$

$$\omega_7 = -\cos qx + \tan q\alpha\sin qx,\ \ \omega_8 = \cos q\left(1-\alpha\right)(-\cos qx + \tan q\alpha\sin qx).$$

APPENDIX B

$$R_1 = \int_{-\alpha}^{0}\left(\frac{d^2 v_2}{dx^2}\right)^2 dx + \int_{0}^{1-\alpha}\left(\frac{d^2 v_1}{dx^2}\right)^2 dx, \quad R_2 = \int_{-\alpha}^{0}\frac{d^2 v_2}{dx^2}dx + \int_{0}^{1-\alpha}\frac{d^2 v_1}{dx^2}dx,$$

$$\gamma_1 = C_2 L + \frac{C_1^2 L}{D\hat{\Delta}^2}R_1,\ \ \gamma_2 = \frac{LC_9^2}{D\hat{\Delta}^2}R_1 + \frac{LC_9^2}{D\hat{\Delta}}R_4,$$

$$\gamma_3 = -P_9 L + \frac{2C_1 C_9 L}{D\hat{\Delta}^2}R_1 + \frac{C_1 C_9 L}{D\hat{\Delta}}R_4.$$

REFERENCES

1. S.A. Ambartsumyan and G.E. Bagdasaryan, (1996), Electroconductive Plates and Shells in Magnetic Field, p.288, Nauka, Moscow (in Russian).
2. S.A.Ambartsumian, M. Belubekyan , (1991), “Some problems of electromagnetoelasticity of plates”. Yerevan, Yerevan State University Publishing House, Yerevan (in Russian), p.144.
3. Anton, S. R. and Sodano H.A. (2007). A review of power harvesting using piezoelectric materials (2003-2006), Smart Mater. Struct., Vol. 16(3), R1-R21.
4. G. E. Bagdasaryan, (1999), Vibrations and Stability of Magnetoelastic Systems, p. 435, Yerevan State University Publishing House, Yerevan (in Russian).
5. Bauer, S., (2006), Piezo-, pyro- and ferroelectrets: soft transducer materials for electromechanical energy conversion, IEEE Transactions on Dielectrics and Electrical Insulation, 13(5), pp. 953 – 962.
6. Beeby, S. P.; Torah, R. N.; Tudor, M. J.; Glynne-Jones, P.; ODonnell, T.; Saha, C. R. & Roy, S. (2007). A micro electromagnetic generator for vibration energy harvesting, J. Micromech. Microeng., Vol.17, 12571265.
7. Blystad, L.-C. J.; Halvorsen, E. and Husa, S. (2008). Simulation of a MEMS Piezoelectric Energy Harvester Including Power Conditioning and Mechanical Stoppers. Technical Digest, PowerMEMS 2008, Sendai, Japan, November 2008, 237-240.
8. Blystad, L.-C. J., Halvorsen, E. & Husa, S. (2010). Piezoelectric MEMS energy harvesting systems driven by harmonic and random vibrations, IEEE Trans. Ultrason., Ferroelect., Freq. Contr., Vol. 57(4), 908-919.
9. Borisenok, V. A., Koshelev, A. S. and Novitsky, E. Z., (1996), Pyroelectric materials for converters of pulsed ionizing radiation energy into electric power, Bulletin of the Russian Academy of Sciences, Physics, 60(10), pp. 1660 –1662.

10. Di Salvo F. J., (1999), Thermoelectric cooling and power generation, Science 285, 703-6.
11. Erturk A. & D. J. Inman (2008). Issues in mathematical modeling of piezoelectric energy harvesters. Smart Mater. Struct. 17, paper # 065016.
12. Gnuni V.Ts., (2006) The stability of beam with two arbitrarily but symmetrical support locations under the action of following forces, Proceeding of National Academy of Science of Armenia, Mechanics, v.59, 1, pp. 25-30.
13. Hasanyan D., Gao J., Wang Y., Viswan R., Li M., Shen Y., Li J. and Viehland D., (2012). Theoretical and experimental investigation of magnetoelectric effect for bending-tension coupled modes in magnetostrictive-piezoelectric layered composites, J. Appl. Phys. 112, 013908 .
14. Jeon Y B, Sood R, Jeong J H and Kim S. G., (2005), MEMS power generator with transverse mode thin film PZT Sensors Actuators A 122 16–22.
15. Kim S, Clark W W and Wang Q. M. (2005), Piezoelectric energy harvesting with a clamped circular plate: analysis J. Intell. Mater. Syst. Struct. 16 847–54
16. Krommer M. and Irschik H., (2000). A Reissner-Mindlin-type plate theory including the direct piezoelectric and pyroelectric effect. Acta Mechanica 141, 51-69 .
17. Librescu L, Hasanyan D., Qin Z. & Ambur D.R., (2003), Nonlinear magnetothermoelasticity of anisotropic plates immersed in a magnetic field. Journal of Thermal Stresses Volume 26, Issue 11-12.
18. Namli O. C. and Taya M., (2011), Design of Piezo-SMA Composite for Thermal Energy Harvester Under Fluctuating Temperature, Journal of Applied Mechanics, v.78.
19. Paradiso J. A. and Starner T. (2005), Energy Scavenging for Mobile and Wireless Electronics, Pervasive Computing, IEEE, vol. 4, pp. 18-27.
20. Poulin G., Sarraute E. and Costa F. (2004), Generation of electric energy for portable devices: comparative study of an electromagnetic and a piezoelectric system. Sensors Actuators A 116 461–71.
21. Rogacheva N. N., (2010), Asymmetrically Laminated Piezoelectric Bars, Journal of Applied Mathematics and Mechanics, vol. 74, pp. 1009-1027.
22. Roundy S, Steingart D, Frechette L, Wright P and Rabaey J, (2004), Power sources for wireless sensor networks Lect. Notes Comput. Sci. 2920 1–17.
23. Sebald G., Guyomar D. and Agbossou A., (2009), On thermoelectric and pyroelectric energy harvesting, Smart Mater. Struct. 18 , 125006.
24. Sodano, H. A., Simmers, G. E., Dereux, R., and Inman,D. J., (2007). Recharging batteries using energy harvestedfrom thermal gradients, Journal of Intelligent Material Systems and Structures, 18, pp. 3 – 10.
25. Ujihara, M., Carman, G. P., and Lee, D. G., (2007), Thermal energy harvesting device using ferromagnetic materials, Applied Physics Letters, 91, p.093508.
26. Xie J., Mane X. P., Green C. W., Mossi K. M. and Leang K. K., (2009), Performance of Thin Piezoelectric Materials for Pyroelectric Energy Harvesting, Journal of Intelligent Material Systems and Structures, vol. 21, pp. 243-249.

About authors:

Gevorg Y. Bagdasaryan – Institute of Mechanics National Academy of Science of Armenia; **E-mail: gevorgb@rau.am**

Armanj D. Hasanyan, Davresh J. Hasanyan – Department of Aerospace Engineering, Ann Arbor, Michigan, USA; **E-mail: dhasanya@vt.edu**

Received 09.06.2015